Online Resource 1: Supplementary Information

Phonon Scattering and Thermal Resistance Allocation in β-Silicon Nitride Nanofilms under Large Temperature Gradients

Thermal Functional Materials — anonymous review copy

S1 Model dimensions and numerical conventions

Two independent nonequilibrium *ab initio* molecular dynamics (NEAIMD) trajectories define the layer-temperature field. Periodic-crystal phonons supply the isothermal response functions. The material thickness, internal center-to-center interval, and cell length including vacuum describe distinct geometric ranges. The local-temperature mapping uses the internal layer coordinates and the frequencies, group velocities, and temperature-dependent rates of a fixed periodic reference lattice. Calculations retain full numerical precision; displayed values are rounded by physical quantity. Input dimensions are retained at higher precision in Table S1 for reproducibility.

Table S1. Model dimensions and numerical conventions.

Quantity	Value or definition
Film composition	60 Si + 80 N; 126 mobile atoms
Section-defined thickness	2.818043 nm; 20 occupied sections
Internal analysis interval	1.831728 nm; layers 4–17; 14 centers
Cell length including vacuum	3.099847 nm
Periodic reference lattice	a = 0.765885 nm; c = 0.292453 nm
Initial film lattice	a = 0.737640 nm; normal repeat = 0.281804 nm
Periodic reference cell volume	$1.4856393 \times 10^{-28}$ m^3; 14 atoms
Transport sampling	14 × 14 × 29; 5684 full-zone points; 42 branches
Reference phonon	Reduced wave vector q = (0, 0, 3/29); branch 3; frequency f = 4.258905 THz
Reference-mode scales	Normal group velocity v_z = 10.728801 km s^{-1}; wavelength λ = 2.827046 nm

The wavelength follows from the periodic reference c parameter and reduced wave vector. Its 2.827 nm value differs by approximately 0.32% from the section-defined film thickness of 2.818 nm. Temperature mapping at the fixed reference lattice compares the response of the same phonon population at the different layer temperatures.

Angular frequencies in the ShengBTE output BTE.omega are read in rad ps^{-1} and converted to THz using $f = \omega/(2\pi)$. Calculations combine heat capacity, lifetime, velocity, and volume using the International System of Units (SI). The all-mode sum retains the actual squared normal velocities over the full wave-vector mesh.

S2 Layer temperatures and temporal blocks

Both independent trajectories use steps 18000–29960 inclusive, giving 11961 temperature records. Fig. S1 retains the actual means of the 14 internal layers. Linear fits summarize the gradients, whereas the scattering and conductivity mappings use the individual layer means.

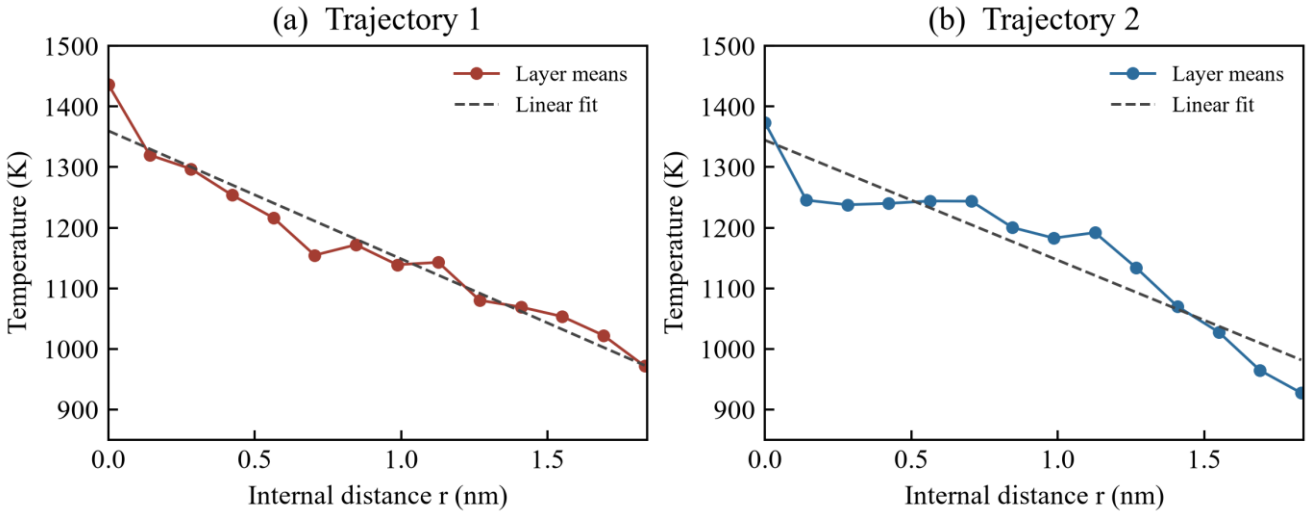


Fig. S1 Internal layer means and linear fits for trajectories 1 in a and 2 in b. The internal hot-side layer center defines r = 0

The selected window is also divided into four nonoverlapping temporal blocks of approximately 3 ps each. Table S2 reports the endpoint drop and fitted gradient in each block. These blocks describe temporal variation within each trajectory; the two separate trajectories are the units of independent replication.

Table S2. Temperature statistics by temporal block.

Trajectory / block	Step interval	ΔT (K)	|∇T| (K nm^{-1})
1 / 1	18000–20990	327.84	182.6
1 / 2	20991–23980	582.48	254.7
1 / 3	23981–26970	448.27	222.8
1 / 4	26971–29960	499.85	185.2
2 / 1	18000–20990	415.90	179.8

Trajectory / block	Step interval	ΔT (K)	|∇T| (K nm⁻¹)
2 / 2	20991–23980	477.29	189.0
2 / 3	23981–26970	432.72	207.5
2 / 4	26971–29960	458.37	215.8

S3 Sensitivity to scattering integration broadening

At 1200 K, the ShengBTE broadening scale is set to 0.8, 1.0, and 1.2 while keeping the force constants, 14 × 14 × 29 transport mesh, and other controls unchanged. Fig. S2 compares the reference-mode contribution and all-mode *c*-axis conductivity in the relaxation-time approximation (RTA) relative to the scale-1.0 baseline.

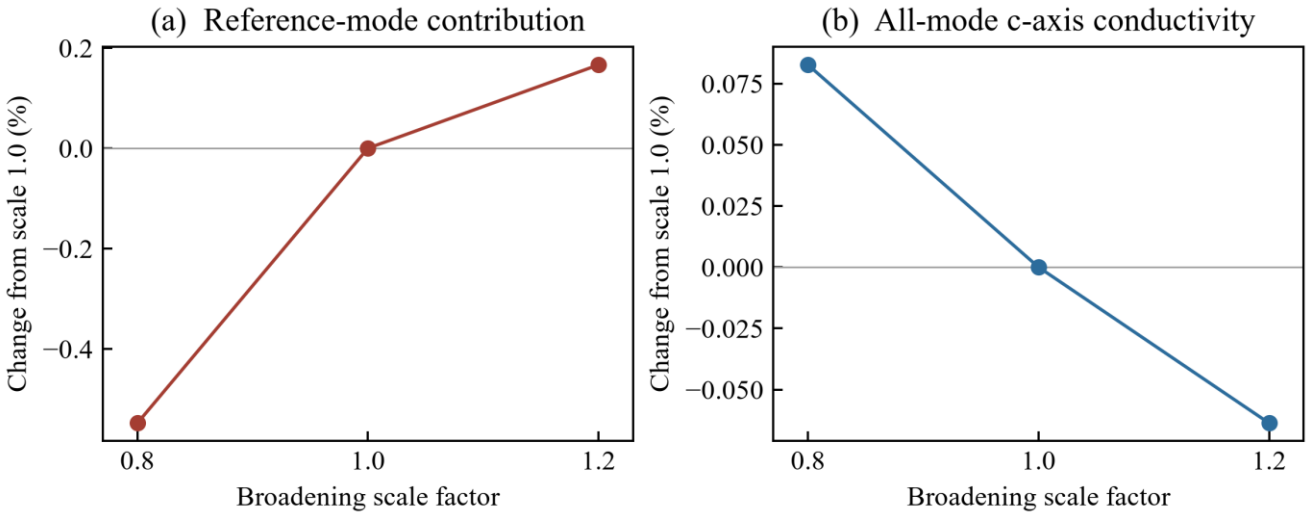


Fig. S2 Broadening sensitivity of the reference-mode contribution in a and all-mode normal conductivity in b at 1200 K. Vertical axes give percentage changes from the baseline

Table S3. Scattering-integration broadening sensitivity at 1200 K.

Scale	Γ^{3ph} (ps⁻¹)	τ_{total} (ps)	κ_{mode} (W m⁻¹ K⁻¹)	κ_c (W m⁻¹ K⁻¹)
0.8	0.07240	13.77	0.02585	38.81
1.0	0.07200	13.85	0.02600	38.78
1.2	0.07188	13.87	0.02604	38.75

Relative to scale 1.0, the reference-mode contribution changes by −0.548% and +0.166%, while the all-mode conductivity changes by +0.083% and −0.064%. The largest change in the reference-mode three-phonon rate is 0.553%. The conductivity and rate metrics therefore quantify their respective responses over this tested broadening interval.

Conductivity uses the total lifetime $\tau_{total} = 1/(\Gamma^{3ph} + \Gamma^{iso})$, whereas $\tau^{3ph} = 1/\Gamma^{3ph}$ describes three-phonon relaxation alone. The total lifetime and modal contribution in Table S3 use the same combined-rate definition.

S4 Density of states integration and mesh comparison

The 21^3, 31^3, and 41^3 meshes use the same periodic structure and second-order force constants. Native linear tetrahedron integration in Phonopy gives the density of states over 0–36 THz with a 0.01 THz output interval. Atomic projections are summed by element, with target integrals of 18, 24, and 42 states per cell for Si, N, and the total. The symbols g_{Si}, g_N, and g_{total} denote the Si-projected, N-projected, and total phonon densities of states (DOS). The normalized cumulative mode count is the cumulative distribution function (CDF) of the phonon density of states. The L1 difference integrates the absolute difference between two DOS curves.

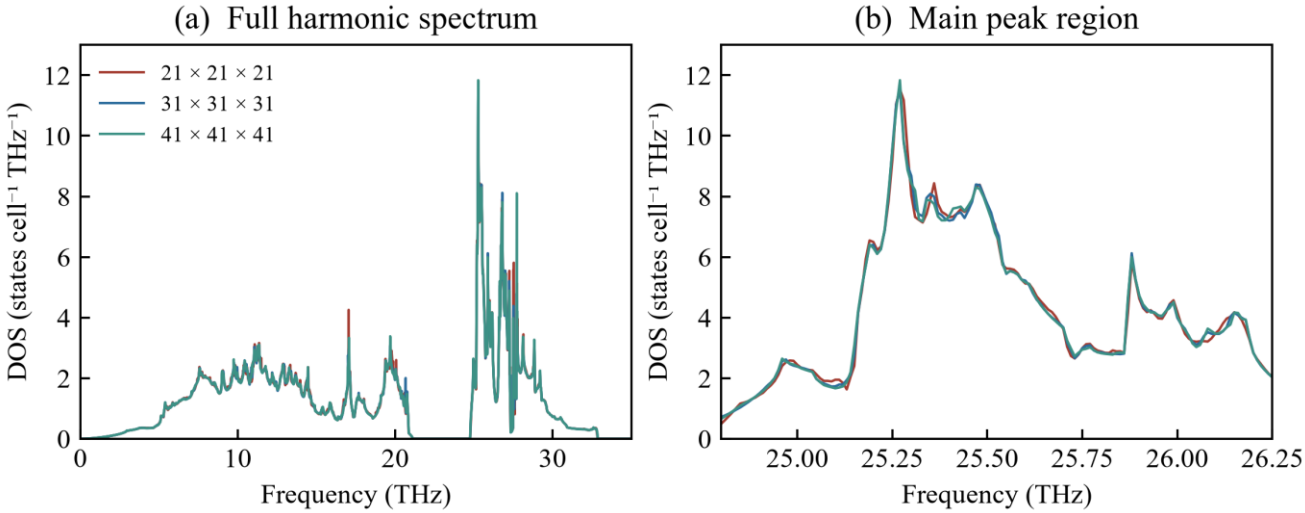


Fig. S3 Total density of states on the three meshes. Panel a shows the complete frequency range and b enlarges the principal peak

Table S4. Density-of-states numerical integrals.

Mesh	**$\int g_{Si}$ df**	**$\int g_N$ df**	**$\int g_{total}$ df**
21^3	18.001	24.021	42.022
31^3	18.002	23.981	41.983
41^3	17.998	24.011	42.009

Table S5. Density-of-states mesh differences.

Mesh change	L1 / 42 (%)	max |ΔCDF| / 42 (%)	Peak-height change (%)
$21^3 \rightarrow 31^3$	3.715	0.105	0.084
$31^3 \rightarrow 41^3$	1.968	0.075	2.486

The L1 metric integrates the absolute density-of-states difference over frequency. The cumulative difference is obtained by integrating each DOS before subtraction. Refinement from 31^3 to 41^3 gives a maximum normalized cumulative difference of 0.075% and a peak-height change of 2.486%, distinguishing the integrated spectral weight from the local peak response.

S5 Information entropy with equal sampling windows

The 49 trajectories form 18 thermal-state groups. The equal-window check uses local steps 20000–29960; these correspond to global steps 50000–59960 for continuation trajectories. Temperature, speed, and potential each have 9961 samples, while adjacent-step potential differences have 9960. Species means over mobile atoms are formed at each time step before fixed-bin probabilities and entropies are evaluated. Thermal ordering is evaluated with Spearman's rank coefficient ρ_S. Agreement between windows is evaluated with Pearson's coefficient r_P and the entropy difference ΔH, defined as equal-window minus selected-window entropy.

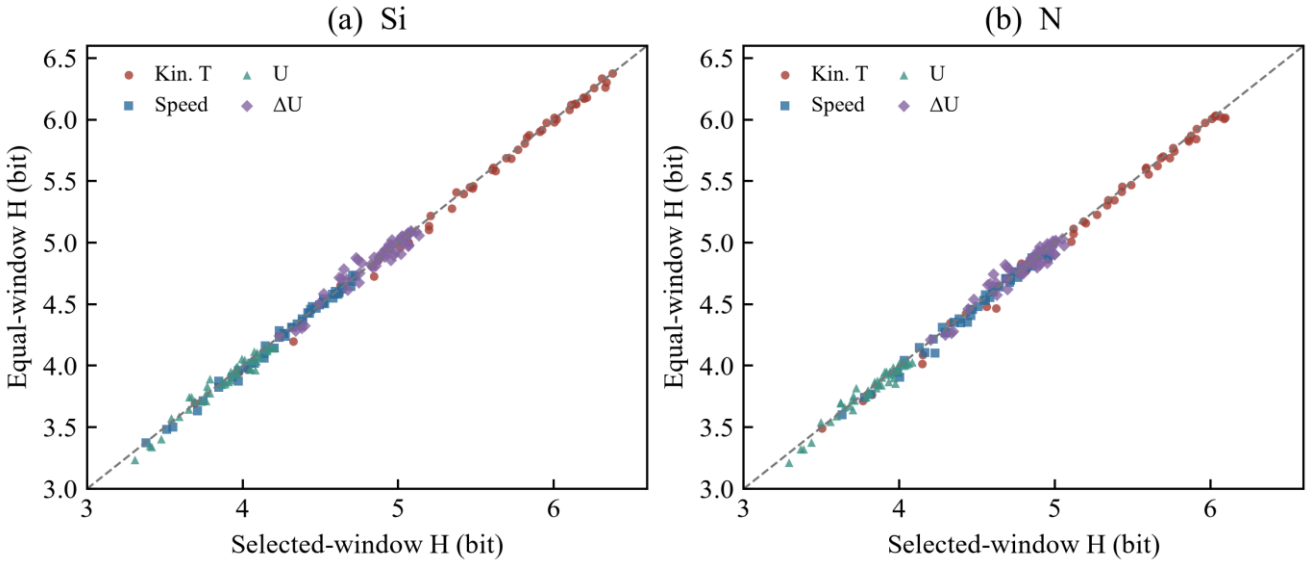


Fig. S4 Per-trajectory comparison of selected-window and equal-window entropy for Si in a and N in b. Dashed lines denote equality; symbols distinguish kinetic temperature (Kin. T), speed, potential U, and adjacent-step potential change ΔU

Table S6. Thermal ordering and per-trajectory entropy agreement.

Element / signal	ρ_s with T	r_P between windows	Mean ΔH (bit)	Max |ΔH| (bit)
Si / Kin. T	1.000	0.999	-0.023	0.126
Si / Speed	0.998	0.997	-0.016	0.099
Si / U	1.000	0.980	-0.009	0.112
Si / ΔU	0.992	0.963	0.002	0.149
N / Kin. T	0.998	0.998	-0.027	0.155
N / Speed	0.998	0.995	-0.020	0.127
N / U	1.000	0.977	-0.007	0.119
N / ΔU	0.981	0.960	0.002	0.142

Here ρ_s is the Spearman coefficient between 18 equal-window group-mean entropies and their actual window-mean temperatures. The Pearson coefficient r_P compares the two entropy estimates across 49 trajectories. ΔH is equal-window minus selected-window entropy. The thermal-ordering coefficients span 0.981–1.000, and the largest absolute mean shift is 0.027 bit.

Bin widths for kinetic temperature, speed, potential, and adjacent-step potential change are 10 K, 0.01 nm ps^{-1}, 0.01 eV, and 0.001 eV, respectively. Each signal uses fixed bin boundaries across temperatures.

S6 Transport integration and accompanying data

All modal conductivity contributions are summed within each layer before inversion to obtain ρ^{ref}. Trapezoidal integration is applied between adjacent centers. The hot-half boundary is $\ell/2$; an interval crossing that midpoint is split using linear resistivity interpolation. Table S7 summarizes the spatial mapping and internal integration for the two trajectories.

Table S7. Internal resistance and endpoint contrasts.

Metric	Trajectory 1	Trajectory 2
Endpoint ΔT (K)	464.60	446.07
$I^{\exists ph}$ hot-to-cold decrease (%)	33.4	33.6
κ_{mode} cold / hot	1.496	1.501

Metric	Trajectory 1	Trajectory 2
κ^{ref} cold / hot	1.492	1.496
R_A (10^{-11} m² K W⁻¹)	4.569	4.572
Hot-half share (%)	53.83	53.58
ℓ / R_A (W m⁻¹ K⁻¹)	40.09	40.07

Spatial spectra sum modal contributions into 0.75 THz bins and divide by the bin width. Frequency integration recovers all-mode conductivity and precedes spatial resistivity integration. The accompanying CSV files provide layer temperatures, rates, modal contributions, the all-mode reference, and the 13 resistance increments.

Accompanying numerical tables

Table S8. Contents of accompanying numerical tables.

Dataset	Contents
Isothermal transport	19 temperatures; reference mode and all-mode conductivities
Layer mapping	28 trajectory–layer states and 26 interval increments
Broadening sensitivity	Three scale factors at 1200 K
DOS integration	21^3, 31^3, 41^3 spectra and integral comparisons
Temporal statistics	Eight disjoint temperature blocks
Information entropy	Eight curves, 18 groups, and 49-trajectory comparisons
Vibration–potential amplitudes	56 element–layer–trajectory root-mean-square (RMS) states

Definitions follow the Methods section of the main text. Phonon methods are described by Togo and Tanaka, Scripta Materialia 108, 1–5 (2015), https://doi.org/10.1016/j.scriptamat.2015.07.021, and Li et al., Computer Physics Communications 185, 1747–1758 (2014), https://doi.org/10.1016/j.cpc.2014.02.015.

Symbols and Abbreviations

Table S9. Symbols and abbreviations.

Symbol or abbreviation	Definition
T, T_i, T(r)	temperature; layer-i kinetic temperature; actual temperature field
r, ℓ, z	internal hot-to-cold coordinate; internal center-to-center length; film-normal direction
a, c; Γ, A	crystal axes; Brillouin-zone center and axial high-symmetry point
K_i, f_i, k_B	layer kinetic energy; dynamical degrees of freedom; Boltzmann constant
μ, q, λ	phonon wave-vector/branch label; wave vector; wavelength
ω_μ, f_μ, $\hbar$	angular frequency; ordinary frequency; reduced Planck constant
Γ_μ, Γ^{3ph}, Γ^{iso}, τ_μ	total rate; three-phonon rate; natural-isotope rate; total lifetime
C_μ, x_μ, $v_{\mu,z}$, N_q, V_c	mode heat capacity; dimensionless frequency; normal velocity; full-zone point count; periodic-cell volume
$\kappa_{\mu,zz}$, κ_{zz}^{RTA}, κ_{zz}^{ref}	single-mode normal contribution; all-mode RTA conductivity; local-temperature conductivity reference
map, ref	superscripts for mapped modal quantities and the all-mode periodic-crystal reference
K_{zz}, G_σ, σ, f	conductivity spectral density; Gaussian kernel; frequency standard deviation; ordinary frequency
u, h, K_h, w_μ, W, b	logarithmic rate coordinate; bandwidth; logarithmic-coordinate kernel; modal counting weight; positive-frequency total weight; frequency group
p_b(Γ;r), p_Γ, F_{high}	group rate density; total rate density; conditional high-frequency mode-count fraction
P10, P50, P90	count-weighted 10th percentile, median, and 90th percentile across modes
ρ^{ref}, R_A^{ref}, $\Delta R_{A,i}$	reference thermal resistivity; cumulative area-normalized reference resistance; interval increment
S_D, S_U, S_V, $S_{\Delta U}$, S_X	spectral densities of displacement, relative electrostatic potential, velocity, adjacent-step potential change, and a general signal X
R_X, $\mathscr{F}$, t, t_0	autocorrelation; Fourier transform; time lag; time origin
φ_j, $\bar{\varphi}_{mob}$, $\delta\varphi_j$, α, $n_{\alpha,r}$, u_α	ionic-core potential; mobile-atom instantaneous mean; zero-time-mean relative potential; element; element-layer atom count; layer mean of atomwise potential RMS
H, p_b, n_b, N	Shannon information entropy; bin probability; bin sample count; total sample count
ρ_s, r_P, ΔH	Spearman rank coefficient; Pearson correlation coefficient; equal-window minus selected-window entropy
NEAIMD, AIMD, RTA, DOS, RMS	nonequilibrium *ab initio* molecular dynamics; *ab initio* molecular dynamics; relaxation-time approximation; density of states; root-mean-square
VASP, PAW, PBE	Vienna Ab initio Simulation Package; projector augmented-wave; Perdew–Burke–Ernzerhof